

SOLVING WAVE PROPAGATION WITHIN FINITE-SIZED COMPOSITE MEDIA WITH LINEAR EMBEDDING VIA GREEN'S OPERATORS

V. Lancellotti* and A. G. Tijhuis

Faculty of Electrical Engineering, Eindhoven University of Technology, Den Dolech 2, 5600 MB, Eindhoven, The Netherlands

Abstract—The calculation of electromagnetic (EM) fields and waves inside finite-sized structures comprised of different media can benefit from a diakoptics method such as linear embedding via Green's operators (LEGO). Unlike scattering problems, the excitation of EM waves within the bulk dielectric requires introducing sources *inside* the structure itself. To handle such occurrence, we have expanded the set of LEGO sub-domains — employed to formulate an EM problem — to deal with the inclusion of elementary sources. The corresponding sub-domains (bricks) play the role of “generators” in the equivalent model. Moreover, if a source is “turned off”, as it were, the enclosing brick can be utilized as a numerical “probe” to sample the EM field. In this paper, we present the integral equations of LEGO modified so as to accommodate generator/probe bricks. Numerical results are provided which demonstrate the validity and the efficiency of the approach.

1. INTRODUCTION AND MOTIVATION

The need for computing the electromagnetic (EM) fields radiated by sources in the presence of composite media (e.g., piecewise homogeneous dielectrics) arises in several engineering applications such as dielectric waveguides and devices, antenna arrays, frequency selective surfaces, to name but a few examples. As real-life structures are finite and oft-times their size is commensurate with the wavelength, a full-wave solution of Maxwell's equations with some numerical method is generally required. In fact, over the past fifty years the Method of Moments (MoM) [1] has been routinely used. It is notorious, though, that turning integral equations (IEs) into a weak form through

Received 14 June 2012, Accepted 6 July 2012, Scheduled 12 July 2012

* Corresponding author: Vito Lancellotti (v.lancellotti@tue.nl).

the standard MoM leads to full and possibly large system matrices. Among the strategies contrived to mitigate the ensuing computational burden, we solely mention domain decomposition methods (DDMs) in tandem with various kinds of macro basis functions [2–7], because these techniques relate to the main topic of our paper.

Initially applied to the scattering off aggregates of metallic objects [7], linear embedding via Green’s operators (LEGO) is a DDM which relies on the conceptual separation of the local (geometrical and material) complexities from the multiple scattering that occurs in a cluster of bodies or between parts of a single structure. In view of said feature, LEGO has also been employed for solving scattering problems that involve composite and diverse media [8–10].

Taking one step forward, we have recently extended LEGO to the calculation of EM fields and waves inside composite (dielectric) media. Unlike scattering problems in which an object is usually illuminated by an external field, launching EM waves within a bulk dielectric requires placing sources *inside* the structure itself. Thus, we have introduced a new type of LEGO sub-domains (bricks) which are devised to embed elementary sources (Fig. 1): Because of their function, we refer to such bricks as “generators.” Still, if necessary, a source can be thought of as “turned off”; then, the enclosing brick can serve as a numerical “probe” to sample the EM field at the source location or, more generally, any other point within the brick. In light of LEGO modularity, not only is the addition of generator/probe bricks straightforward but it also marginally affects the IE which describes a problem. Hence, we can adopt the numerical strategy based on Arnoldi basis functions

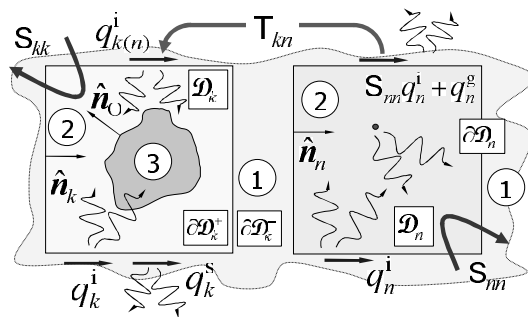


Figure 1. For defining passive (\mathcal{D}_k) and generator (\mathcal{D}_n) LEGO bricks along with scattering and transfer operators, plus equivalent incident ($q_{k,n}^i$), scattered ($q_{k,n}^s$) and generator (q_n^g) currents. The labels ①, ② and ③ denote background, host and object medium, respectively.

(ABFs) [8, 9] without substantial changes.

The remaining of the paper is organized as follows. In Section 2 we derive the system of LEGO IEs in the presence of generator/probe bricks. Then, in Section 3 we elaborate on the description of a generator brick and the calculation of the fields within a probe brick. Finally, numerical results concerning the validation and application of the approach are discussed in Section 4.

2. FORMULATION WITH LEGO REVISITED

When the solution of a complicated EM problem involving composite media is tackled with LEGO, one begins by defining N_D bricks \mathcal{D}_k , $k = 1, \dots, N_D$, whose EM behavior is rigorously described in terms of scattering operators \mathbf{S}_{kk} . The latter — which account for the geometrical and material complexities that may exist inside \mathcal{D}_k — are determined separately for each brick at the beginning [7, 8].

More specifically, by virtue of the surface equivalence principle [11] we introduce various types of equivalent electric (\mathbf{J}) and magnetic (\mathbf{M}) surface current densities over $\partial\mathcal{D}_k^-$. As emphasized in Fig. 1, such currents are set against $\partial\mathcal{D}_k$, though they exist *within* the background medium ①. With these positions, in the quite general case when a brick embeds a source the relevant constitutive equation reads

$$q_k^s = \mathbf{S}_{kk} q_k^i + q_k^g, \quad q_k^{s,i,g} = \begin{bmatrix} \sqrt{\eta_1} \mathbf{J}_k^{s,i,g} \\ -\mathbf{M}_k^{s,i,g} / \sqrt{\eta_1} \end{bmatrix}, \quad \eta_1 = \sqrt{\frac{\mu_1}{\varepsilon_1}}, \quad (1)$$

where the superscripts ‘s’, ‘i’ and ‘g’ are catchy reminders for scattered, incident and generator, respectively. The equivalent current density q_k^g — the distinctive attribute of a “generator” brick — is to account for the fields radiated by the source[†] (e.g., an elementary dipole) localized inside \mathcal{D}_k . In fact, when no sources are enclosed in \mathcal{D}_k , then q_k^g vanishes and (1) reduces to the usual constitutive equation for passive bricks [7, Eq. (7)]. Still, it ensues from (1) that q_k^s may be non-null even if q_k^i vanishes — which corresponds to the special case of a solitary generator brick in the background medium and in the absence of external sources.

To proceed we need to define $N_D(N_D - 1)$ transfer operators \mathbf{T}_{kn} which we employ to describe the multiple scattering that occurs among the bricks, as hinted at in Fig. 1. By definition, \mathbf{T}_{kn} is to produce additional equivalent incident currents on $\partial\mathcal{D}_k^-$ as a result of scattered

[†] We will show in Section 3 that the effect of the abrupt change in the material properties at the interface $\partial\mathcal{D}_k$ is included in q_k^g as well. Conversely, it is quite superfluous to embed a source in a brick filled with a medium ② whose properties are the same as the background’s.

currents induced on $\partial\mathcal{D}_n^-$, viz.,

$$q_{k(n)}^i = \mathbb{T}_{kn} q_n^s, \quad n \neq k, \quad (2)$$

where the subscript ‘ $k(n)$ ’ means “incident currents on \mathcal{D}_k due to sources on \mathcal{D}_n .” Notice that, consistently with \mathbb{T}_{kn} being unaffected by the bricks’ content, (2) is the same as [7, Eq. (13)]. In the light of (1), (2), apparently $q_{k(n)}^i$ is not only caused by contrast currents inside \mathcal{D}_n (or even right on $\partial\mathcal{D}_n$), but also by independent elementary sources, when \mathcal{D}_n happens to be a generator brick.

The last step towards a full-wave formulation of the problem consists of combining all the bricks electromagnetically. To this end let B_g the set of indices pertaining to the generator bricks in the model. A closer look at (1), (2) suggests that the equations governing the EM behavior of a structure modelled with N_D bricks are

$$q_n^s = \begin{cases} \mathbb{S}_{nn} q_{n,\text{tot}}^i + q_n^g, & n \in B_g, \\ \mathbb{S}_{nn} q_{n,\text{tot}}^i, & n \notin B_g, \end{cases} \quad q_{k,\text{tot}}^i = \sum_{n \neq k}^{N_D} \mathbb{T}_{kn} q_n^s, \quad (3)$$

where $q_{k,\text{tot}}^i$ contains the total incident electric and magnetic current densities over $\partial\mathcal{D}_k^-$ and is defined similarly to $q_k^{s,i,g}$ in (1). Plugging the expression of q_n^s into the second of (3) and performing a little algebra allows writing the functional equation succinctly as

$$(\mathbb{I} - \mathbb{T} \mathbf{diag}\{\mathbb{S}_{nn}\}) q_{\text{tot}}^i = \mathbb{T} q^g, \quad (4)$$

with q_{tot}^i an N_D -element symbolic column vector storing $q_{k,\text{tot}}^i$, and q^g likewise a column vector with non-null entries q_l^g , $l \in B_g$. Besides, \mathbb{T} is a symbolic square matrix of transfer operators [8] and \mathbb{I} a suitable diagonal matrix of identity operators.

Once q_{tot}^i has been computed, we obtain the scattered currents through the first of (3). More importantly, thanks to the physical meaning of $q_{k,\text{tot}}^i$, q_k^s , and paying due regard to the orientation of the normal $\hat{\mathbf{n}}_k$ (see Fig. 1), the difference $q_{k,\text{tot}}^i - q_k^s$ yields the total (twisted) tangential electric and magnetic fields over $\partial\mathcal{D}_k$.

Except for the different form of the forcing term, (4) bears close resemblance to [8, Eq. (5)]. Confessedly, (4) may be made even more general by adding to $\mathbb{T}q^g$ a vector q^i that takes into account any true sources *outside* the structure, but here we will not explore this circumstance any further. By contrast, we observe that in principle all the N_D bricks may simultaneously be generators.

3. GENERATOR AND PROBE BRICKS

In this section we work out an expression for the generator current q_k^g , and we elaborate on the calculation of the fields inside a brick. Both

tasks are most involved if the brick of concern embeds one or more objects. Thereby, for the time being we content ourselves with the case of a brick without inclusions, as the rightmost one in Fig. 1.

3.1. Calculation of the Generator Current

In [8] by posing suitable surface integral equations on $\partial\mathcal{D}_k$ we derived the 2-by-2 scattering operator \bar{S}_{Jk} of the interface. The purpose of \bar{S}_{Jk} is to link scattered and incident currents on both sides of $\partial\mathcal{D}_k$. In symbols, the latter reads

$$\begin{bmatrix} q_{J1,k}^s \\ q_{J2,k}^s \end{bmatrix} = \begin{bmatrix} S_{J11,k} & S_{J12,k} \\ S_{J21,k} & S_{J22,k} \end{bmatrix} \begin{bmatrix} q_{J1,k}^i \\ q_{J2,k}^i \end{bmatrix}, \quad (5)$$

where with evident notation the integer number in the subscript of an equivalent current tells whether it belongs to the background (①) or the host (②) medium (see Fig. 1). Such currents are defined similarly to the ones we introduced in (1).

Now, the effect of a source inside \mathcal{D}_k is exactly reproduced by an equivalent current $q_{J2,k}^i$ on $\partial\mathcal{D}_k^+$ that satisfies (cf. [7])

$$P_{22,k}^i q_{J2,k}^i = F_{t2,k}^i, \quad F_{t2,k}^i = \begin{bmatrix} \mathbf{0} \\ \sqrt{\eta_2} \mathbf{H}_{t2,k}^i \end{bmatrix}, \quad \eta_2 = \sqrt{\frac{\mu_2}{\varepsilon_2}}, \quad (6)$$

where $P_{22,k}^i$ is the *propagator* detailed in Table 1, and $\mathbf{H}_{t2,k}^i$ represents the incident magnetic field in medium ②. More precisely, $P_{22,k}^i$ (a

Table 1. Definition of propagator $P_{22,k}^i$ used in (6), (7).

$G_2(R)$ is the 3-D scalar Green's function in medium ②.
The unit normal $\hat{\mathbf{n}}_k$ to $\partial\mathcal{D}_k$ points <i>inward</i> \mathcal{D}_k (Fig. 1).
NOMENCLATURE
$G_2(R) = \exp(-jk_2 R)/(4\pi R), \quad R = \mathbf{r} - \mathbf{r}' , \quad k_2 = \omega\sqrt{\varepsilon_2\mu_2},$
$\underline{I}_s = \underline{I} - \hat{\mathbf{n}}_k \hat{\mathbf{n}}_k, \quad \nabla_s = \nabla - \hat{\mathbf{n}}_k \hat{\mathbf{n}}_k \cdot \nabla, \quad \nabla'_s = -\nabla_s$

$\partial\mathcal{D}_k^+ \rightarrow \partial\mathcal{D}_k^+$ (from incident currents to incident fields), $\mathbf{r} \in \partial\mathcal{D}_k^+$
$(P_{22,k}^i)_{11} = -j \int_{\partial\mathcal{D}_k^+} d^2r' \left[k_2 G_2(R) \underline{I}_s + \frac{1}{k_2} \nabla_s G_2(R) \nabla'_s \right] \cdot$
$(P_{22,k}^i)_{12} = -\text{P.V.} \int_{\partial\mathcal{D}_k^+} d^2r' \nabla'_s G_2(R) \times \underline{I}_s \cdot -\frac{1}{2} \hat{\mathbf{n}}_k \times \underline{I}_s \cdot$
$(P_{22,k}^i)_{21} = \text{P.V.} \int_{\partial\mathcal{D}_k^+} d^2r' \nabla_s G_2(R) \times \underline{I}_s \cdot + \frac{1}{2} \hat{\mathbf{n}}_k \times \underline{I}_s \cdot$
$(P_{22,k}^i)_{22} = -(P_{22,k}^i)_{11}$

2×2 abstract matrix of dyadic operators) acts on equivalent incident currents on $\partial\mathcal{D}_k^+$ to yield incident fields thereon. Since $q_{J2,k}^i$ radiates the actual fields generated by the source towards infinity (and null fields in \mathcal{D}_k), $P_{22,k}^i$ looks formally the same as P_{kk}^s in [7, Table 1]. The actual calculation of $\mathbf{H}_{t2,k}^i$ depends on the nature of the source as well as the shape of $\partial\mathcal{D}_k$. In fact, if the relevant source is an elementary dipole, then $\mathbf{H}_{t2,k}^i$ is nothing but the corresponding magnetic Green's function (in an unbounded medium) evaluated for observation points on $\partial\mathcal{D}_k$.

As a last step, we invert (6) symbolically and insert $q_{J2,k}^i$ into the first row of (5); on comparison with the first of (1) we then obtain

$$\mathbf{S}_{kk} = \mathbf{S}_{J11,k}, \quad q_k^s = \mathbf{S}_{J12,k} (\mathbf{P}_{22,k}^i)^{-1} F_{t2,k}^i, \quad (7)$$

which provide a suitable recipe for characterizing a generator brick. Though a formal result, (7) acquires practical significance in the context of the numerical solution of (4) through the MoM.

3.2. Calculation of the Fields inside a Probe Brick

In order to determine the fields in selected points inside a structure, after solving (4), we can adopt the conceptual expedient of inserting probe bricks in the LEGO model. A probe brick, however, is just a generator which has been turned off, so to speak.

Although not strictly mandatory, such point of view makes it simpler to implement the strategy in a numerical code, because probe bricks can be dealt with pretty much in the same way as generator bricks. In this respect, switched-off generator bricks contribute a zero in the corresponding positions of the vector q^s in (4). Secondly, the relevant scattering operators are already available from (7). Lastly, as the position of the elementary source is already known information, "sampling" the scattered field at the source location is straightforward — which may be enough for some applications.

To see how this is done in practice, we begin by observing that the equivalent current density $q_{J2,k}^s$ (in the light of its definition) is responsible for radiating the *scattered* fields inside a brick. From the second of (5), for a generator brick we then have

$$q_{J2,k}^s = \mathbf{S}_{J21,k} q_{k,\text{tot}}^i + \mathbf{S}_{J22,k} (\mathbf{P}_{22,k}^i)^{-1} F_{t2,k}^i, \quad (8)$$

where $q_{k,\text{tot}}^i$ factors in the effect of the remaining $N_D - 1$ bricks. In this instance, obtaining the *total* fields requires adding the direct contribution of the source inside \mathcal{D}_k . Since the field of a concentrated source is singular at its own location, that point must be excluded. By

contrast, as the source is off inside a probe brick, not only does the rightmost term in (8) vanish, but more importantly, $q_{J2,k}^s$ is all we need to compute the fields in *any* point of \mathcal{D}_k .

We now apply the reaction theorem [11] to an unbounded region with the properties of the host medium ②. (Recall that we are allowed to “fill” the space outside \mathcal{D}_k with any medium deemed convenient, inasmuch as $q_{J2,k}^s$ radiates no fields in there.) To this purpose, we choose the states as follows:

State (a) The sources are the equivalent scattered surface current densities $\mathbf{J}_{2,k}^s$ and $\mathbf{M}_{2,k}^s$ on $\partial\mathcal{D}_k^+$, as given by (8).

State (b) The source is an elementary electric (magnetic) dipole of unit moment $\hat{\mathbf{p}}_e$ ($\hat{\mathbf{p}}_h$), and located at the point $\mathbf{r} \in \mathcal{D}_k$ where the value of the electric (magnetic) field is desired.

In keeping with the very idea of a probe brick, the dipoles relevant to state (b) above are just a mathematical tool for sampling the scattered field inside \mathcal{D}_k . Therefore, $\hat{\mathbf{p}}_{e,h}$ should not be confused with the true source, although they may all share the same location, as argued at the beginning of this section.

To finalize our derivation, we equate the reactions to arrive at

$$\hat{\mathbf{p}}_e \cdot \mathbf{E}_k^s(\mathbf{r}) = \int_{\partial\mathcal{D}_k} d^2r' [\mathbf{E}\{\hat{\mathbf{p}}_e\} \cdot \mathbf{J}_{2,k}^s - \mathbf{H}\{\hat{\mathbf{p}}_e\} \cdot \mathbf{M}_{2,k}^s], \quad (9)$$

$$-\hat{\mathbf{p}}_h \cdot \mathbf{H}_k^s(\mathbf{r}) = \int_{\partial\mathcal{D}_k} d^2r' [\mathbf{E}\{\hat{\mathbf{p}}_h\} \cdot \mathbf{J}_{2,k}^s - \mathbf{H}\{\hat{\mathbf{p}}_h\} \cdot \mathbf{M}_{2,k}^s], \quad (10)$$

where $\mathbf{E}\{\hat{\mathbf{p}}_{e,h}\}$ ($\mathbf{H}\{\hat{\mathbf{p}}_{e,h}\}$) signifies the electric (magnetic) field produced at \mathbf{r}' by the dipole with moment $\hat{\mathbf{p}}_{e,h}$. The Cartesian components of the scattered field inside \mathcal{D}_k ensue by setting $\hat{\mathbf{p}}_{e,h} \in \{\hat{\mathbf{x}}, \hat{\mathbf{y}}, \hat{\mathbf{z}}\}$ in (9), (10) in succession.

As regards the practical implementation of (9), (10), we notice that the fields $\mathbf{E}\{\hat{\mathbf{p}}_{e,h}\}$, $\mathbf{H}\{\hat{\mathbf{p}}_{e,h}\}$ can be computed by the same piece of code that provides $\mathbf{H}_{t2,k}^i$ (and, though not used, $\mathbf{E}_{t2,k}^i$ as well) in (6), as long as the elementary source of concern is a dipole. Again, this is a consequence of medium ② being reciprocal.

4. NUMERICAL RESULTS

Since to solve (4) numerically we employ the same procedure described thoroughly in [8, 10], the interested Reader is kindly referred to those works for the necessary details. Here we just recapitulate the essential points to lay the groundwork for the numerical results discussed below.

To begin with, (4) is turned into a weak form by applying the MoM (in Galerkin's form) with Rao-Wilton-Glisson (RWG) functions [12]. More precisely, the currents $q_k^{s,i,g}$, $q_{k,tot}^i$, are all expanded on a set of $2N_F$ RWG functions associated with the N_F edges of the 3-D triangular-facet mesh which models a brick's boundary. If a brick encloses an object, then N_O RWG functions are likewise introduced over the object's surface (also see [7]). The algebraic system resulting from (4) (size $2N_F N_D \times 2N_F N_D$) is to be solved for the vector of current coefficients $[q_{tot}^i]$. The latter is expressed as a superposition of n_A Arnoldi basis functions (ABFs), namely, $[q_{tot}^i] = \sum_{s=1}^{n_A} [\psi_s] a_s$. Since $n_A \ll 2N_F N_D$, this change of basis effectively compresses the original system, which can then be inverted via LU factorization. The convergence properties of the ABFs are investigated to a great extent in [9] and literature cited therein.

4.1. Example of Validation

In order to check that the numerical solution of (4) has been correctly implemented, we consider the toy problem (a dielectric slab embedding elementary sources) whose LEGO model is shown in Fig. 2. In particular, we want to make sure that the symmetry relations dictated by the reaction theorem [11] are actually fulfilled.

To this purpose, we model the dielectric slab by means of $N_D = 2$ generator/probe bricks of cubical shape. (Other geometrical and simulation data are given in the caption of Fig. 2.) Next, we define two states as follows:

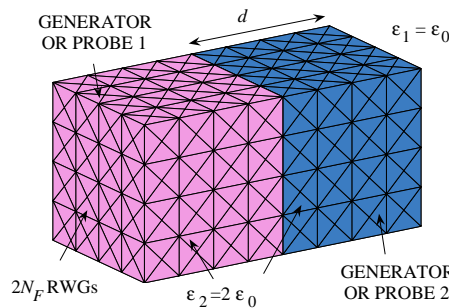


Figure 2. For validation of generator/probe LEGO bricks: a dielectric slab (ϵ_2), immersed in free space (ϵ_1), is modelled with $N_D = 2$ cubic bricks. An elementary dipole of moment \mathbf{p}_e or \mathbf{p}_h is located at each brick's center. *Data:* $d = 1$ cm, $2N_F = 1152$, $n_A = 30$, $f \in [5, 7]$ GHz.

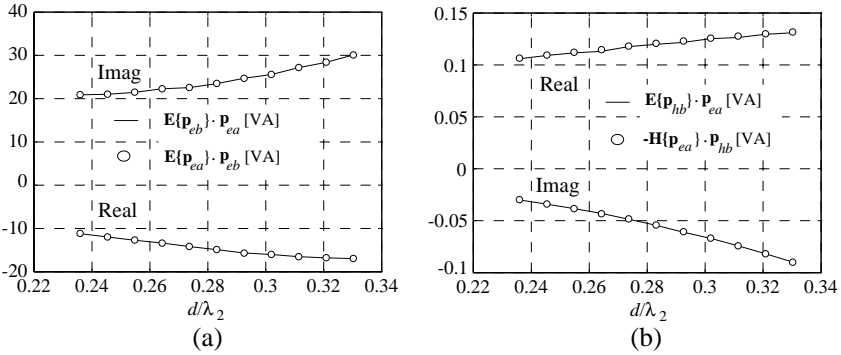


Figure 3. Validation of generator/probe bricks: (a) the reaction $\mathbf{E}\{\mathbf{p}_{eb}\} \cdot \mathbf{p}_{ea}$ (—) is compared to the reaction $\mathbf{E}\{\mathbf{p}_{ea}\} \cdot \mathbf{p}_{eb}$ (○); (b) the reaction $\mathbf{E}\{\mathbf{p}_{eb}\} \cdot \mathbf{p}_{ea}$ (—) is compared to the reaction $-\mathbf{H}\{\mathbf{p}_{ea}\} \cdot \mathbf{p}_{hb}$ (○). *Data:* $\mathbf{p}_{ea} = \mathbf{p}_{eb} = 0.01\hat{\mathbf{y}}$ Vm, $\mathbf{p}_{hb} = 0.01\hat{\mathbf{z}}$ Am, $1/\lambda_2 = f\sqrt{\varepsilon_2\mu_0}$.

State (a) The source is an elementary electric dipole of moment \mathbf{p}_{ea} located at the center of \mathcal{D}_1 (leftmost brick in Fig. 2).

State (b) The source is an elementary electric (magnetic) dipole of moment \mathbf{p}_{eb} (\mathbf{p}_{hb}) located at the center of \mathcal{D}_2 .

Finally, an application of the reaction theorem to whole space provides us with the two conditions

$$\mathbf{E}\{\mathbf{p}_{eb}\} \cdot \mathbf{p}_{ea} = \mathbf{E}\{\mathbf{p}_{ea}\} \cdot \mathbf{p}_{eb}, \quad \mathbf{E}\{\mathbf{p}_{eb}\} \cdot \mathbf{p}_{ea} = -\mathbf{H}\{\mathbf{p}_{ea}\} \cdot \mathbf{p}_{hb}, \quad (11)$$

where the notation complies to (9), (10). The quantities on both sides of the relations in (11) — as computed by our code — are compared in Fig. 3 as a function of the electrical distance (in medium ②) between the two dipoles. As can be seen, the two sets of curves for each case are perfectly overlapped for all practical purposes. From a numerical standpoint, the two states are realized by assuming either \mathcal{D}_1 or \mathcal{D}_2 to be a generator and the other brick a probe, as proposed in Section 3.2.

4.2. Example of Application

Let us apply LEGO to the problem of wave propagation inside two composite structures (Fig. 4) which consist of the same finite-size dielectric slab (medium ②) immersed in free space (medium ①). One or two waveguides are patterned within the bulk dielectric by means of cylindrical holes (medium ③) that are etched in selected positions.

We commence by “dicing” the slab into $N_D = 105$ cubical bricks with various content and function, as required by the relevant EM

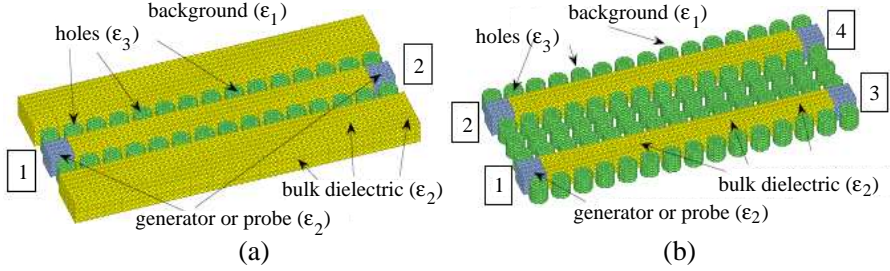


Figure 4. Modelling two composite dielectric structures with LEGO: (a) single waveguide and (b) two parallel waveguides comprised of “defects.” (For visualization’s sake the surface of the bricks that embed the cylindrical holes is not displayed.)

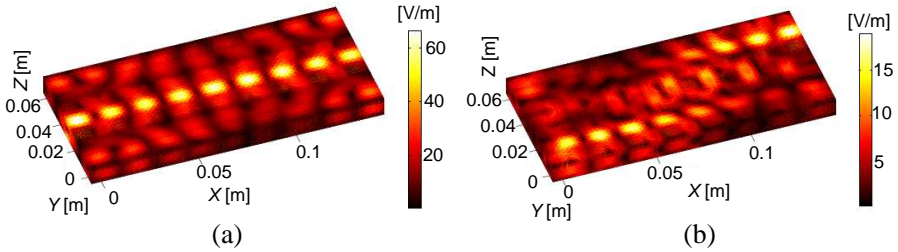


Figure 5. Computed $|\mathbf{E} \times \hat{\mathbf{n}}|$ for the structures of Fig. 4: (a) single waveguide with generator brick at port 1 (port 2) on (off); (b) two waveguides with generator brick at port 1 (ports 2, 3, 4) on (off).

problem. For instance, to model the single waveguide of Fig. 4(a) we employ 2 generator/probe bricks, 30 bricks with holes and 73 bulk dielectric bricks. By contrast, the two waveguides shown in Fig. 4(b), are modelled via 4 generator/probe bricks, 75 bricks with holes and only 26 bulk dielectric bricks. We also assume all the sources to be the elementary magnetic current $\mathbf{M} = 10^{-3} \hat{\mathbf{x}} \delta^{(3)}(\mathbf{r} - \mathbf{r}_0) \text{ V/m}^2$, with \mathbf{r}_0 the center of the generator/probe bricks; therefore, we need to define just one type of generator bricks.

In both problems the bricks’ edge is 1 cm, the holes’ diameter and height is 0.8 cm, and we choose the working frequency as $f = 6.3 \text{ GHz}$. The three media are not magnetic and have permittivities $\varepsilon_1 = \varepsilon_3 = \varepsilon_0$, $\varepsilon_2 = 11\varepsilon_0$. Lastly, for the numerical solution with MoM and ABFs, $2N_F = 1152$ and $N_O = 498$ (this is the number of RWGs set over a hole’s surface to represent electric and magnetic currents thereon [7]).

As an example of results, plotted in Fig. 5 is the distribution of

the total twisted electric field ($|\mathbf{E} \times \hat{\mathbf{n}}|$) over the visible part of the bricks' surface. These values are obtained with port 1 energized and the generators at the remaining ports turned off. The electric field components registered by the probe bricks at port 2 (single waveguide) and port 4 (two waveguides) are listed in Table 2.

From Fig. 5(a) the alternative occurrence of peaks and troughs (characteristic of a guided wave) is quite evident along the central row of "defects". In this region the electric field also seems to take on its largest values. Farther off in the y -direction and on either side of the waveguide, close to the sharp material boundaries of the slab, two other waves may be spotted. Nevertheless, the maximum field level appears to be roughly half the value of the maximum in the waveguide. Hence, we are led to conclude that the two rows of holes are able to effectively confine the field in the y -direction, while vertical confinement is afforded by classical total internal reflection.

From Fig. 5(b) we notice that the wave launched at port 1 dies out as it travels towards port 3, while a specular wave gradually appears in the parallel (not excited) waveguide. Most likely, the two waveguides are coupled as a consequence of the non-perfect isolation brought in by the holes. Apparently, contrary to one's expectations, stacking more rows of holes does not improve the wave confinement (at least at this frequency) inasmuch as the maximum field level in Fig. 5(b) is about one third of the maximum value in Fig. 5(a).

For the two problems in Fig. 4 the algebraic counterpart of (4) is

Table 2. Computed electric fields inside probe bricks.

Structure	Port	E_x [V/m]	E_y [V/m]	E_z [V/m]
Fig. 4(a)	2	$0.138 - 0.282j$	$0.243 + 0.044j$	$-0.046 - 0.002j$
Fig. 4(b)	4	$-0.245 + 0.050j$	$0.001 - 0.059j$	$-2.68 - 1.91j$

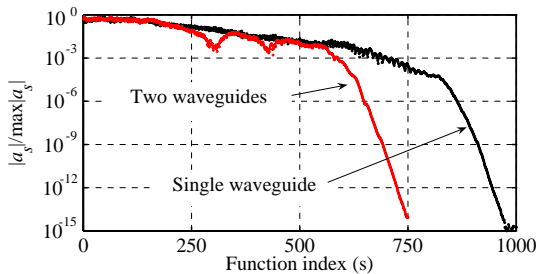


Figure 6. Convergence pattern of the current coefficients a_s in the basis of the ABFs (cf. [8, Eq. (17)]) for the problems of Fig. 4.

a linear system of rank $2N_F N_D = 120960$ which is reduced by using $n_A = 1000$ and $n_A = 750$ ABFs respectively. The distributions of the Arnoldi coefficients a_s are plotted in Fig. 6 versus s : Apparently, regardless of the problem, the a_s 's decrease exponentially after a threshold. As the convergence properties, though, are presumably related to the spectrum of $\mathbf{T} \mathbf{diag}\{\mathbf{S}_{nn}\}$ in (4) [9, Section 4.3], the onset of exponential decay occurs at different indices most assuredly because the two LEGO models comprise unlike numbers of the three basic brick types. In truth, for a given level of accuracy one would expect the two-waveguide problem to require more ABFs than the other one, on the grounds that in the former the multiple scattering between the bricks must be more intricate due to the presence of many more embedded objects. However, this hypothesis may not be entirely justified, as the "objects" in question here are actually holes ($\varepsilon_3 < \varepsilon_2$). In conclusion, predicting which structure should exhibit the faster convergence is not simple without comparing the eigenvalues of $\mathbf{T} \mathbf{diag}\{\mathbf{S}_{nn}\}$ (which is outside the scope of the paper). But then, since the effect of the generator bricks only shows in the forcing term of (4), we can rightfully claim that in this respect the presence of generators does not affect the convergence pattern of a given structure. Yet, it is true that if the source is changed, the ABFs have to be determined over again, as they are obtained from $\mathbf{T}q^s$ in (4) (cf. [8]).

On the positive side, the modularity of LEGO makes it efficient to tackle the problems of Fig. 4 (and many similar more in succession) in that some intermediate results can be re-utilized, thus saving on computational time. For a start, we need to compute the scattering operators of the three brick types only once. Then, we can re-use them regardless of a brick's actual position in the model. Next, if a limited translational symmetry can be invoked, the transfer operators are known to come in groups of identical specimens [7]. The practical consequence is that the number N_T of \mathbf{T}_{kn} 's we have to calculate is most likely far smaller than $N_{T,\max} = N_D(N_D - 1)$. For the two slabs of Fig. 4, $N_T = 376$ whereas $N_{T,\max} = 10920$. What's more, since the models of Fig. 4 solely differ for the content of the bricks, we determine the minimum number of transfer operators only the first time.

For completeness, we mention that the time spent[‡] to compute the \mathbf{T}_{kn} 's is about 98 s, whereas it took 23 s on average to generate a single ABFs.

[‡] Calculations run on Linux-based x86.64 work-station equipped with an Intel Xeon 2.66-GHz processor and 8-GB RAM.

5. CONCLUSION

In the context of the LEGO method, we have discussed the definition and usage of generator/probe bricks to account for sources inside a composite dielectric structure. Basically, a generator/probe brick is no different than an ordinary one, except for its role in the model. Since formulating a problem with LEGO ultimately boils down to combining various types of bricks, the functional equation stays essentially the same. As a result, the numerical solution can be carried out with the MoM and the ABFs as before. Actually, we have demonstrated that the insertion of generator bricks is inconsequential for the convergence properties of the ABFs. Finally, we have shown how scattering and transfer operators — the building blocks of LEGO — can be re-utilized to tackle multiple problems while saving on computational time.

ACKNOWLEDGMENT

This research was partly supported by the TU/e project No. 36/363450, and carried out in the framework of the MEMPHIS project (www.smartmix-memphis.nl). The Authors would like to thank an anonymous Reviewer whose remarks helped them improve the manuscript.

REFERENCES

1. Harrington, R. F., *Field Computation by Moment Methods*, MacMillan, New York, 1968.
2. Yuan, H.-W., S.-X. Gong, Y. Guan, and D.-Y. Su, "Scattering analysis of the large array antennas using the synthetic basis functions method," *Journal of Electromagnetic Waves and Applications*, Vol. 23, Nos. 2–3, 309–320, 2009.
3. Li, M. K. and W. C. Chew, "Wave-field interaction with complex structures using equivalence principle algorithm," *IEEE Trans. Antennas Propag.*, Vol. 55, 130–138, Jan. 2007.
4. Mittra, R. and K. Du, "Characteristic basis function method for iteration-free solution of large method of moments problems," *Progress In Electromagnetics Research B*, Vol. 6, 307–336, 2008.
5. Xiao, G., J.-F. Mao, and B. Yuan, "A generalized surface integral equation formulation for analysis of complex electromagnetic systems," *IEEE Trans. Antennas Propag.*, Vol. 57, 701–710, Mar. 2009.

6. Ylä-Oijala, P. and M. Taskinen, “Electromagnetic scattering by large and complex structures with surface equivalence principle algorithm,” *Waves in Random and Complex Media*, Vol. 19, 105–125, Feb. 2009.
7. Lancellotti, V., B. P. de Hon, and A. G. Tijhuis, “An eigencurrent approach to the analysis of electrically large 3-D structures using linear embedding via Green’s operators,” *IEEE Trans. Antennas Propag.*, Vol. 57, 3575–3585, Nov. 2009.
8. Lancellotti, V., B. P. de Hon, and A. G. Tijhuis, “Scattering from large 3-D piecewise homogeneous bodies through linear embedding via Green’s operators and Arnoldi basis functions,” *Progress In Electromagnetics Research*, Vol. 103, 305–322, Apr. 2010.
9. Lancellotti, V. and A. G. Tijhuis, “Convergence properties of a diakoptics method for electromagnetic scattering from 3-D complex structures,” *Progress In Electromagnetics Research M*, Vol. 24, 127–140, May 2012.
10. Lancellotti, V., B. P. de Hon, and A. G. Tijhuis, “Wave scattering from random sets of closely spaced objects through linear embedding via Green’s operators,” *Waves in Random and Complex Media*, Vol. 21, 434–455, Aug. 2011.
11. Rothwell, E. J. and M. J. Cloud, *Electromagnetics*, CRC Press, London, 2001.
12. Rao, S. M., D. R. Wilton, and A. W. Glisson, “Electromagnetic scattering by surfaces of arbitrary shape,” *IEEE Trans. Antennas Propag.*, Vol. 30, 409–418, May 1982.